HHS Public Access

Author manuscript

Kidney Int. Author manuscript; available in PMC 2016 January 01.

Published in final edited form as:

Kidney Int. 2015 July ; 88(1): 95–108. doi:10.1038/ki.2015.102.

Macrophage and epithelial cell H-ferritin expression regulates renal inflammation

Subhashini Bolisetty[1,*], **Abolfazl Zarjou**[1,*], **Travis D. Hull**[1], **Amie Traylor**[1], **Anjana Perianayagam**[1], **Reny Joseph**[1], **Ahmed I Kamal**[1], **Paolo Arosio**[2], **Miguel P Soares**[3], **Viktoria Jeney**[4,5], **Jozsef Balla**[4,5], **James F. George**[1], and **Anupam Agarwal**[1,6]

[1]Nephrology Research and Training Center, Division of Nephrology, Department of Medicine, University of Alabama at Birmingham, Birmingham, Alabama, USA

[2]Dipartimento Materno Infantile e Tecnologie Biomediche, University of Brescia, Brescia, Italy

[3]Inflammation Laboratory, Instituto Gulbenkian de Ciência, Oeiras, Portugal

[4]Department of Medicine, University of Debrecen, Debrecen, Hungary

[5]MTA-DE Vascular Biology, Thrombosis and Hemostasis Research Group, Hungarian Academy of Sciences, Debrecen, Hungary

[6]Department of Veterans Affairs, Birmingham, Alabama, USA

Abstract

Inflammation culminating in fibrosis contributes to progressive kidney disease. Crosstalk between the tubular epithelium and interstitial cells regulates inflammation by a coordinated release of cytokines and chemokines. Here we studied the role of heme oxygenase-1 (HO-1) and the heavy subunit of ferritin (FtH) in macrophage polarization and renal inflammation. Deficiency in HO-1 was associated with increased FtH expression, accumulation of macrophages with a dysregulated polarization profile, and increased fibrosis following unilateral ureteral obstruction in mice; a model of renal inflammation and fibrosis. Macrophage polarization *in vitro* was predominantly dependent on FtH expression in isolated bone marrow-derived mouse monocytes. Utilizing transgenic mice with conditional deletion of FtH in the proximal tubules (*FtH*PT−/−) or myeloid cells (*FtH*LysM−/−), we found that myeloid FtH deficiency did not affect polarization or accumulation of macrophages in the injured kidney compared to wild-type (*FtH*+/+) controls. However, tubular FtH deletion led to a marked increase in pro-inflammatory macrophages. Furthermore, injured kidneys from *FtH*PT−/− mice expressed significantly higher levels of inflammatory chemokines and fibrosis compared to kidneys from *FtH*+/+ and *FtH*LysM−/− mice. Thus, there are differential effects of FtH in macrophages and epithelial cells, which underscores the critical role of FtH in tubular-macrophage crosstalk during kidney injury.

Correspondence: Anupam Agarwal M.D., Division of Nephrology, THT 647, University of Alabama at Birmingham, 1900 University Blvd., Birmingham, AL 35294, agarwal@uab.edu, Phone (205) 996 6670, Fax (205) 996 6650.

*The first two authors contributed equally to this work

Disclosure

All the authors declared no competing interests.

Keywords

Ferritin; inflammation; fibrosis; macrophage polarization; acute kidney injury

Introduction

The kidney is a complex organ that is involved in a myriad of vital processes, which is made possible by a well-orchestrated milieu of different cell types. Damage to the kidney parenchyma leading to loss of kidney function results in significantly increased morbidity and mortality. In addition, infiltration of inflammatory cells at early stages in the injured kidneys, followed by tubulointerstitial fibrosis are common pathologic features of acute injury-mediated progressive kidney disease (1–3). The pathogenesis of progressive kidney disease is remarkably complex and includes activation of multiple pathways involved in inflammation and oxidative stress (4–7). Following injury, a cascade of events is initiated that leads to tubular epithelial injury and activation of tissue-resident and infiltrating macrophages. This cascade is the result of a coordinated action of cytokines/chemokines and reactive oxygen species. Furthermore, a single insult to the kidney also heightens the risk for the development of chronic kidney disease (CKD) (6,8,9).

Recent seminal work in this field has demonstrated that two distinct responses ensue following injury. First, the injured tubular epithelium triggers a robust local response by inducing several survival and regenerative pathways including upregulation of anti-oxidants and recruitment of inflammatory cells through release of chemokines and cytokines (6,10–15). Of the anti-oxidants, we and others have demonstrated a protective role for the expression of heme oxygenase-1 (HO-1) and the heavy subunit of ferritin (FtH) during acute kidney injury (16–22). HO-1 catalyzes the breakdown of heme to carbon monoxide, bile pigments and ferrous iron. The iron released from this reaction is converted to a ferric form by FtH and securely stored in the ferritin shell thereby limiting iron-mediated oxidative stress (23). In addition to the oxidative changes within the tubular epithelium, proximal tubular cells also increase their production and secretion of chemokines that recruit and activate inflammatory cells (14,24–26).

The influx of these inflammatory cells, predominantly macrophages, comprise the second response to injury. Macrophages progressively accumulate in the injured kidney in response to chemokines and cytokines such as monocyte chemoattractant protein 1 (MCP-1), colony stimulating factor 1 (CSF-1) and Interleukin 6 (IL-6) and play a central role in propagation or resolution of injury (15,27–30). Early studies demonstrated that macrophage infiltration correlates with the severity of kidney injury in humans and animals, suggesting a pathogenic role for these cells (31–33). In fact, animal studies concluded that depletion of macrophages prior to injury led to amelioration of renal fibrosis while adoptive transfer of macrophages aggravated the injurious response (34–37). However, recent evidence suggests that while macrophage depletion in the early stages following injury is protective, depletion of macrophages during the resolution phase of injury delays recovery (24,38,39). This apparently contradictory role for macrophages can be explained by their heterogeneity for the expression of different proteins that enable cytotoxic or cytoprotective functions (40–

43). This differential expression pattern allows for macrophages to be classified into two subclasses with polar functions: termed classically activated M1 and alternatively activated M2. M1 macrophages are characterized by the expression of high levels of pro-inflammatory cytokines and increased production of reactive oxygen and nitrogen species. M2 macrophages are anti-inflammatory and produce metabolic intermediates such as ornithine and polyamines that enable tissue remodeling and homeostasis (41,44). In this context, HO-1 is robustly expressed by M2 macrophages, conferring potent anti-inflammatory properties (45–48). This dichotomous polarization of macrophages underscores their diverse roles in regulating tissue injury and repair, providing exciting avenues to potentially modulate responses following injury.

Injury to the kidney parenchyma and inflammation are interdependent and form a vicious cycle where tubular injury facilitates macrophage influx and vice versa. This often perpetuates the development of fibrosis, an adverse complication compromising kidney function. It is therefore increasingly evident that dissecting the signaling mechanisms during cross-talk between parenchymal tubular cells and inflammatory cells is crucial for development of novel therapeutic interventions. We addressed the hypothesis that expression of HO-1 and FtH in proximal tubular epithelial cells and macrophages are involved in the mechanisms leading to exacerbation or resolution of inflammation-mediated fibrosis. To test this hypothesis, we utilized a well-established unilateral ureteral obstruction model (UUO), characterized by oxidative stress and inflammatory-mediated fibrosis, in order to elucidate the relative contribution of macrophages versus the kidney microenvironment in resolution of injury. We used transgenic mice with global deletion of *HO-1* or conditional deletion of *FtH* in renal proximal tubules and/or myeloid cells, two cytoprotective anti-oxidant proteins that influence recovery and resolution following renal injury. While the mechanisms of injury and repair were determined using UUO as a model, the results from these studies may be applicable to inflammatory diseases where oxidative stress and inflammation play a determinant pathogenic role.

Results

HO-1 deficiency leads to increased inflammation following unilateral ureteral obstruction

In order to characterize the differential accumulation of immune cells following injury, cells were isolated from the contralateral and obstructed kidneys and analyzed by flow cytometry (Figure 1A). In agreement with previous reports (49), we first demonstrated that two populations of immune cells (CD45+) reside in the uninjured (contralateral) kidney (Figure 1). The predominant population, which has been defined as dendritic cells, is phenotypically characterized as F4/80^{hi}CD11b^{lo} while a second smaller population, defined as macrophages, is characterized as F4/80^{lo}CD11b^{hi} phenotype. As previously reported in a model of AKI induced by ischemia-reperfusion injury (49), we demonstrated a specific and significant increase in the macrophage (CD11b^{hi}F4/80^{lo}) population after UUO, compared to the contralateral kidney (CD11b^{high}F4/80^{lo}; 19.27±5.5% versus 4.80±0.65%) (Figure 1, supplemental figure 1). However, we observed a reduced proportion of dendritic cells (CD11b^{lo}F4/80^{high}; 18.34±4.09% versus 49.8±10.3%) in the obstructed kidneys when compared to contralateral kidneys (Figure 1, supplemental figure 1). In addition,

granulocytes (neutrophils) were identified and excluded from the analysis based on their expression of Ly6C and GR-1. Intra-renal macrophages were further characterized based on Ly6C and CD11c expression (Figure 1B). Ly6C is a surface marker expressed by a subset of circulating monocytes that expand in the context of inflammation and then traffic to the site of injury (50,51). It is also expressed on pro-inflammatory M1 macrophages in the kidney and the heart (49,52). We found an increased proportion of $Ly6C^+$ macrophages in kidneys subjected to UUO compared to contralateral kidneys (Figure 1B). In addition, we found that the $Ly6C^-$ macrophages exhibit a distinct $CD11c^+$ phenotype, which is characteristic of the tissue-resident or tissue-reparative M2 macrophages (53,54).

We have previously demonstrated that *HO-1*$^{-/-}$ mice demonstrate significantly higher levels of $F4/80^+$ cells and fibrosis following UUO compared to wild-type mice (55). Upon further characterization of the $F4/80^+$ cells, we found that global HO-1 deficiency was associated with increased number of macrophages and dendritic cells in the injured kidneys (Figure 1C). Of these macrophages, there was an increase in the number of $Ly6C^+CD11C^+$ macrophages (Figure 1C, Supplemental Figure 1A–B). Of note, the contralateral kidneys of *HO-1*$^{-/-}$ mice also demonstrated a significant increase in the accumulation of macrophages and dendritic cells (Supplemental Figure 1A–C).

We identified the phenotype of macrophages in the injured kidneys of *HO-1*$^{-/-}$ and *HO-1*$^{+/+}$ mice after UUO. Consistent with previous reports, macrophages isolated from the injured kidneys of *HO-1*$^{+/+}$ mice demonstrated a time-dependent phenotypic expression profile. These macrophages were predominantly M1 (*iNOS*, *TNF*α) at 2 days following injury whereas they expressed M2 marker (*mannose receptor*) at 7 days post injury (Figure 1D). However, HO-$1^{+/+}$ macrophages isolated at different timepoints after injury did not demonstrate a significant change in arginase expression. On the contrary, the *HO-1*$^{-/-}$ macrophages exhibited a dysregulated expression profile with decreased expression of M1 markers on day 2 and increased expression of M2 markers on day 2 and day 5. At day 7, *mannose receptor*, an M2 marker was markedly elevated in both *HO-1*$^{+/+}$ and *HO-1*$^{-/-}$ mice kidneys, but was significantly lower in *HO-1*$^{-/-}$ kidneys (Figure 1D).

Heavy chain ferritin regulates macrophage polarization in vitro

In order to further investigate the dysregulated polarization in *HO-1*$^{-/-}$ macrophages, we isolated bone marrow derived monocytes of *HO-1*$^{+/+}$ and *HO-1*$^{-/-}$ mice and polarized them to M1 or M2 macrophages in vitro using IFNγ or IL-4, respectively (Figure 2A). Corroborating our in vivo data, HO-1 deficient macrophages demonstrated increased propensity to polarize (increased iNOS and arginase expression) when compared to stimulated HO-$1^{+/+}$ macrophages (Figure 2B, supplemental figure 2A). Interestingly, HO-1 deficient macrophages demonstrated higher levels of FtH (Figure 2B). To determine whether FtH was responsible for increased polarization, we pre-treated *HO-1*$^{-/-}$ macrophages with deferoxamine, an iron chelator, to decrease FtH expression. Inhibition of FtH in the *HO-1*$^{-/-}$ macrophages reduced iNOS and arginase expression following stimulation with cytokines (Figure 2C, supplemental figure 2B). In order to verify that polarization was dependent on FtH and not iron, we pre-treated *HO-1*$^{+/+}$ macrophages with apoferritin (ferritin shell made up of heavy and light subunits but devoid of iron) to increase

FtH expression. In the presence of apoferritin, *HO-1*$^{+/+}$ macrophages responded to cytokines with a significantly increased expression of iNOS and arginase and confirmed the contributory role of FtH in increasing the polarizability of macrophages (Figure 2D, supplemental figure 2C). This was also verified using recombinant FtH (Figure 2E, supplemental figure 2D). Furthermore, mutant FtH that is devoid of ferroxidase activity was also able to induce macrophage polarization, confirming that this process is independent of iron regulation by FtH (Figure 2E). Apoferritin and mutant ferritin also induced expression of HO-1 (Figure 2D–E). Of note, supplementation of by-products of the heme oxygenase reaction (carbon monoxide, biliverdin and bilirubin) also led to decreased expression of FtH and polarizability of HO-1 deficient macrophages (Supplemental Figure 3A). In addition, HO-1 overexpressing macrophages (isolated from humanized BAC transgenic mice expressing HO-1) demonstrated decreased expression of FtH and macrophage polarization markers, an effect that was reversed in the presence of apoferritin (Supplemental Figure 3B).

Myeloid-specific FtH deletion does not alter macrophage polarization following injury in vivo

Given the significance of FtH to mediate macrophage polarization, we hypothesized that deletion of FtH in myeloid cells, including macrophages, would significantly inhibit their polarization in vivo following UUO and thereby reduce inflammation. Of note, global FtH deficiency leads to embryonic lethality and hence we chose to generate targeted FtH deletion mice (56). To this end, we generated mice with myeloid-specific deletion of FtH (*FtH*$^{\mathrm{LysM}-/-}$) by breeding *FtH*$^{lox/lox}$ mice with LysM-Cre mice. Mice with myeloid-restricted FtH deficiency (*FtH*$^{\mathrm{LysM}-/-}$) were born at the expected Mendelian ratio, were viable and fertile, and following six months of observation did not manifest any apparent abnormalities. *FtH*$^{\mathrm{lox/lox}}$ mice were homozygous for the floxed allele and express FtH in macrophages and henceforth will be referred to as *FtH*$^{+/+}$ mice. Deletion of FtH expression in macrophages of *FtH*$^{\mathrm{LysM}-/-}$ mice was confirmed by mRNA and protein expression analysis on bone-marrow derived macrophages (Figure 3A–B). In addition, in vitro macrophage polarization was diminished in the absence of FtH in macrophages (Figure 3C). Interestingly, levels of the light chain of ferritin (FtL) and HO-1 were higher in *FtH*$^{\mathrm{LysM}-/-}$ macrophages (Figure 3C).

In order to determine the significance of FtH deletion in macrophages during injury, we performed UUO on *FtH*$^{+/+}$ and *FtH*$^{\mathrm{LysM}-/-}$ mice and analyzed renal inflammation two days following injury (Figure 3D). The total number of macrophages and dendritic cells were not different in the *FtH*$^{\mathrm{LysM}-/-}$ kidneys when compared to *FtH*$^{+/+}$ kidneys (Figure 3E, Supplemental Figure 4). In addition, there was no significant difference in the number of Ly6C^{+}CD11C^{+} and Ly6C^{+}CD11c$^{\mathrm{lo}}$ macrophages in the myeloid-specific FtH deleted kidneys compared to *FtH*$^{+/+}$ obstructed kidneys. Furthermore, circulating lymphocytes recruited to the kidney (CD62L^{+}) at two days post-injury were not different between the two groups (Figure 3E). These results suggest that recruitment of macrophages to the kidney following injury is not affected by their inability to express FtH.

While macrophage recruitment/proliferation in the injured kidney was not altered by FtH, we next sought to determine the polarization profile of macrophages in the *FtH*$^{+/+}$ and

FtH$^{LysM-/-}$ kidneys after UUO. Intra-cellular staining and flow cytometry revealed that the percentage of macrophages (CD45+CD11b^{high}F4/80^{low}) that expressed TNFα, IL-10 or CD206 was not different between *FtH*$^{+/+}$ and *FtH*$^{LysM-/-}$ mice (Supplemental Figure 5). In addition, two days following UUO, macrophages were isolated from the kidneys and analyzed for the expression of M1 and M2 markers by real-time PCR. While most M1 (*iNOS, TNFα, IL-12*) and M2 (*MRC, IL-4, Ym1, CX3CR1, IL-10*) genes were not differentially expressed in the absence of FtH in the macrophages, only *arginase* (M2) was significantly higher in the absence of FtH (Figure 3F). An increase in HO-1 expression was also observed in macrophages isolated from the *FtH*$^{LysM-/-}$ mice kidneys (Figure 3F). No significant differences in the expression of receptors (CCR4 and CSF-1R) for chemokines (MCP-1 and CSF-1) involved in macrophage recruitment were observed (data not shown).

Proximal tubule FtH deletion exacerbates inflammation following UUO

To elucidate the significance of kidney FtH expression in regulation of inflammation during injury, we performed UUO on transgenic mice deficient in FtH expression only in the proximal tubules of the kidney (*FtH*$^{PT-/-}$) (Figure 4A). We previously demonstrated that these mice display increased susceptibility to AKI (cisplatin nephrotoxicity and glycerol-induced rhabdomyolysis) (22). Two days following UUO, while the number of dendritic cells was not different, macrophage accumulation tended to be higher in *FtH*$^{PT-/-}$ kidneys when compared to *FtH*$^{+/+}$ kidneys (Figure 4B, Supplemental Figure 6). Specifically, there was a significant increase in the inflammatory macrophage subset (Ly6C^{+}CD11C^{+}) with no significant difference in the Ly6C^{+}CD11c^{lo} macrophage subset (Figure 4B). There was also a significant increase in CD62L^{+} macrophages in the *FtH*$^{PT-/-}$ kidneys, suggesting that at least a proportion of the intra-renal macrophages are derived from the circulation and do not arise from in situ proliferation (Figure 4B). In addition, intra-cellular staining and flow cytometry revealed that the percentage of macrophages that expressed TNFα, a M1 marker was significantly higher in the FtH$^{PT-/-}$ kidneys compared to *FtH*$^{+/+}$ kidneys (Supplemental Figure 5). Moreover, there was no significant difference in the percentage of IL-10 or CD206 expressing M2 macrophages between the FtH$^{PT-/-}$ and *FtH*$^{+/+}$ mice (Supplemental Figure 5).

Gene expression analysis of macrophages from the injured kidneys revealed predominant M1 polarization (*TNFα, IL-12*), with very low expression of M2 markers (*arginase, IL-4, Ym1 and CX3CR1*) (Figure 4C). In addition, there were no significant differences in the expression of receptors for CSF-1 and MCP-1 (data not shown). These results underscore the importance of the conducive kidney microenvironment for inflammatory M1 macrophage polarization.

FtH expression in the kidney regulates macrophage recruitment through CSF-1, MCP-1 and IL-6

The characterization of inflammatory cells and their phenotype in the absence of FtH in different cellular compartments following UUO highlighted the importance of the kidney, particularly the proximal tubule epithelial cell, in the regulation of the response to injury. Given that kidney-restricted FtH deletion led to a significant increase in macrophage infiltration, we determined the expression of chemokines in the kidney that are responsible

for their recruitment. While deletion of FtH in the macrophages did not influence chemokine expression, absence of FtH in the proximal tubules led to a significant increase in MCP-1 and CSF-1 (Figure 5). Furthermore, while the pro-inflammatory cytokine, IL-6 was significantly higher, the expression of the anti-inflammatory cytokine, IL-10 was lower in the kidneys of $FtH^{PT-/-}$ mice when compared to $FtH^{+/+}$ mice (Figure 5).

FtH expression modulates fibrosis following UUO

In order to determine the effects of FtH deletion in the development of fibrosis, we performed reversible UUO on cell-specific FtH deficient mice wherein the ureter is briefly clamped for two days followed by clamp removal for five days (Figure 6A). This model allows for the determination of cellular responses that occur in the kidney during the resolution phase of injury. As evident from Figure 6B and 6C, fibrosis was significantly higher in the obstructed kidneys of $FtH^{PT-/-}$ mice. Interestingly, while no significant differences were observed in macrophage accumulation (Figure 3), fibrosis was lower in the kidneys of $FtH^{LysM-/-}$ mice when compared to kidneys of $FtH^{+/+}$ mice (Figure 6B). These results were further corroborated by expression of fibronectin and alpha-smooth muscle actin (Figure 6C). Intriguingly, these effects were also observed in the contralateral kidneys (Supplemental Figure 7).

Discussion

Inflammation is an evolutionary defense mechanism in response to injurious stimuli and infectious agents with the ultimate goal of minimizing injury and enabling repair (57). Hence, it is not surprising that dysregulation of a fundamental mechanism is at the epicenter of numerous pathological conditions. In this regard, macrophages have evolved to play a major role in orchestrating a delicate balance of opposition to noxious stimuli versus assisting in re-establishment of tissue homeostasis (41,42,58).

In this study, we investigated the potential role of FtH in regulating macrophage activation and polarization, and the ensuing extent of injury and fibrosis in a model of inflammation and fibrosis in the kidney. We confirmed that UUO is associated with a renal influx of macrophages in $HO\text{-}1^{-/-}$ mice (55), but we show for the first time that these renal macrophages exhibit deranged polarization. Further in vitro results revealed that HO-1 deficient macrophages have increased levels of FtH and is associated with increased expression of both M1 and M2 specific markers. The increase in these markers was directly attributed to ferritin based on similar results observed in $HO\text{-}1^{+/+}$ macrophages that were supplemented with exogenous recombinant FtH or apoferritin and, additionally a decrease in expression of the same markers in the absence of FtH. Using cell specific transgenic mice, we demonstrate that conditional deletion of FtH in macrophages does not affect influx, chemokine expression, or polarization of macrophages. Of note, the LysM promoter used to generate myeloid-specific FtH deletion is active in macrophages, dendritic cells and granulocytes. However, recent studies indicate that LysM promoter expression is low in $CD11c^{+}$ cells (59). Despite this expression pattern, our studies revealed that there were no differences in influx or accumulation of macrophages and dendritic cells in the obstructed kidneys of $FtH^{LysM-/-}$ mice. In contrast, specific deletion of FtH in proximal tubule

epithelial cells was associated with increased propensity of macrophages to be polarized towards a M1 phenotype, a process that correlates with increased injury and ultimately fibrosis.

We recognize that while the in vitro studies provided mechanistic insight into the polarization of macrophages in a conditioned environment that was predominantly dependent on FtH expression, in vivo studies highlight the complex inflammatory microenvironment and cellular cross-talk that may not be completely reflected in the in vitro state. Furthermore, it is important to recognize that the polarization status may also be influenced by the nature of the cytokines in the systemic circulation.

Ferritin is an ancient molecule traditionally thought to be a storage depot for cytoplasmic iron. This notion has been recently challenged and emerging data suggest that ferritin is responsible for diverse functions that are beyond the scope of merely iron handling. Mitochondrial ferritin and localization of FtH in the nucleus have been described and underscore the cellular function and regulatory mechanisms that may depend on this complex and versatile protein (60–64). Ferritin molecules isolated from vertebrates are composed of two types (heavy [H] and light [L] chain) whose proportion depends on the iron status of the cell, the tissue, and the organ. The H-chain has ferroxidase activity that is essential to prevent cellular damage provoked by reactive oxygen species (65). Increasing evidence suggests a role of ferritin in inflammation (66). Elevated levels of ferritin are observed in multiple autoimmune disorders and it is also generally accepted that serum ferritin is an acute phase reactant (67). While serum ferritin is mainly composed of the iron-poor L chain, the described receptors are specific for the H-chain (68). Additional evidence suggests that FtH has immunomodulatory functions although paradoxical effects have been described. For instance, FtH may have immunosuppressive effects via inhibition of antibody production by B lymphocytes, suppression of Type IV hypersensitivity to induce anergy and stimulation of IL-10 production in lymphocytes (69–71). In addition, lower levels of serum ferritin is associated with an increased risk for human acute kidney injury following cardiopulmonary bypass surgery (72). In contrast, ferritin has also been shown to exert pro-inflammatory effects likely via activation of nuclear factor κB (73). Such an effect is independent of the iron content of ferritin and, perhaps more importantly, induction of pro-inflammatory pathways is independent of L or H chain structure (73). Taken together, although there is strong evidence to suggest an immunomodulatory role for ferritin, it is clear that our understanding of the details of such modulation is in its infancy. Given the fact that prolonged or deranged inflammation is a central mediator of numerous clinical conditions, further research into this area will greatly enhance our understanding of the pathogenesis of such conditions and will provide a platform for novel therapeutic modalities and targets to be identified. To this end we were prompted to further delineate the function(s) that iron and ferritin may have in inflammation.

Our results indicate that overexpression of FtH in macrophages leads to a state of activation that primes these cells to polarize towards the M1 or M2 phenotype depending on the cytokines present in their environment. Increased levels of ferritin are likely the result of elevated levels of free heme as well as, iron and heme containing proteins such as cytochromes that are commonly present during cell injury and death in inflamed tissues.

Herein, we demonstrate that conditional deletion of proximal tubule specific FtH, which leads to increased levels of free iron in the microenvironment that is ingested by phagocytic cells such as macrophages, results in increased M1 macrophage polarization and subsequently perpetuates fibrosis, a common determinant of progressive kidney disease (Figure 7). Proximal tubular deletion of FtH led to increased levels of several pro-inflammatory chemokines such as MCP-1, IL-6, CSF-1 and suppression of IL-10 expression. In addition, a recent study identified IL-6 as a key regulator of UUO-mediated fibrosis by induction of collagen expression (74). The pro-inflammatory and pro-fibrotic role of myeloid-specific FtH was further validated by lower levels of fibrosis in mice that were deficient in macrophage FtH expression.

Interestingly, a recent study demonstrated that while Galectin-3 deletion did not alter macrophage recruitment to the kidneys after UUO, adoptive transfer of Galectin-3 deficient macrophages led to decreased fibrosis through reduced activation/recruitment of myofibroblasts (35). In corroboration with this study, our results also demonstrate that while myeloid-specific FtH deletion does not alter macrophage recruitment, it has a significant impact on fibrosis. Myeloid FtH deletion also led to marked increase in arginase expression, a key enzyme involved in the inhibition of fibrosis (75). The key cellular mediators of fibrosis are myofibroblasts, which can be identified by their expression of α-smooth muscle actin (SMA). These cells are the principal producers of the extracellular matrix and are often found in the tubulointerstitial space following UUO. The origin of these myofibroblasts has generated much debate over the past decade and has led to the identification of multiple sources for these cells during injury. These include, but not limited to, bone marrow-derived, pericyte-derived, and epithelial and endothelial mesenchymal transition (76–78). While the principal aim of this study was to identify tubular-macrophage cross-talk in renal fibrosis and injury, future studies will need to focus on characterizing the mechanism of myofibroblast differentiation in this model. The results from this study not only identify macrophage FtH as an important pro-inflammatory molecule but also highlight the importance of the crosstalk between the injured epithelial cells and macrophages. Such crosstalk is perhaps the ultimate determinant of the extent of injury and the resolution/outcome of inflammation in which FtH plays a central role.

From a clinical perspective, chronic kidney disease (CKD) and end stage renal disease patients commonly demonstrate high levels of serum ferritin (79,80). Circulating ferritin may then lead to higher FtH expression in macrophages and as our results demonstrate, high ferritin levels are associated with “priming” of macrophages. Although these patients have complex and multiple factors that could potentially contribute to changes in macrophage polarization, an evaluation of the macrophage phenotype from patients with CKD and varying levels of ferritin would be of interest.

Taken together, these results for the first time provide evidence that FtH expression regulates macrophage activation and polarization, which are strongly dictated by the inflammatory mediators present in the injured proximal tubule epithelial cells and is both cell and context dependent (Figure 7). These mediators provide essential communication between the injured tissue and activated inflammatory cells that will eventually decide the fate of the inflammatory process and fibrosis. Further investigations in this field are required

to shed more light on clinical conditions that have chronic inflammation as a common denominator with a dedicated focus on targeting FtH expression.

Materials and Methods

Animals

HO-1$^{+/+}$ and *HO-1*$^{-/-}$ male mice (10–14 weeks of age) on a mixed C57BL/6 X FVB background were used in this study. Macrophages isolated from humanized HO-1 BAC transgenic mice (12–14 weeks of age) on a C57BL/6 background were used in this study (81). H-ferritin floxed mice and proximal-tubule specific H-ferritin deleted mice that were previously described were used in this study and referred to as *FtH*$^{+/+}$ and *FtH*$^{PT-/-}$ (22,82). The myeloid-specific H-ferritin deletion mice were generated by breeding FtH$^{+/+}$ mice with LysM-cre transgenic mice and referred to as *FtH*$^{LysM-/-}$. All the FtH transgenic mice used in this study were predominantly on a C57BL/6 background. Adult male *FtH*$^{PT-/-}$ mice (8 weeks of age) were provided acidified water (0.3M ammonium chloride) for 1 week to enhance PEPCK promoter activity in the kidney.

Animal model of renal inflammation and fibrosis

UUO surgery was performed as previously described (55). Mice were anesthetized with inhalation of isoflurane (1.5%). In the UUO group, the left ureter was exposed through a mid-abdominal incision and ligated twice, approximately 1 cm below the renal hilum, using a 4-0 silk suture. Sham operation was done in a similar manner, without ureteral ligation. Mice were harvested after 2, 5 or 7 days following ligation. Reversible UUO was performed by clamping the left ureter with a non-traumatic microvascular clip (5–15 g/mm2, 7 mm S&T Vascular Clamp, Fine Science Tools). The clamp was removed two days after clamping and animals were allowed to recover for 5 days. At the time of harvest, kidneys were analyzed for histopathologic studies, immune cell influx, and gene or protein expression analysis.

Fibrosis

Collagen deposition was measured using picrosirius red as previously described (83). Briefly, kidneys were cut transversely and fixed in 10% buffered formaldehyde, embedded in paraffin and sectioned. The kidney sections were deparaffinized with xylene and then rehydrated in water through graded ethanol washes. The sections were incubated in picrosirius red for 1 hour followed by two washes in acidified water. The sections were then dehydrated, cleared, and mounted in a resinous medium. The area of collagen deposition, stained red by picrosirius red staining, was measured by color image analysis software (Image-Pro Plus, Media Cybernetics).

Isolation and Enrichment of Renal Leukocytes

Leukocytes were isolated as previously described with minor modifications (84). Mice were anesthetized with isoflurane (1.5% in 95% O_2) and perfused with 10 ml of ice-cold saline through the left ventricle after median thoracotomy to clear the kidney of leukocytes in the circulation. The contralateral and obstructed kidneys were explanted, washed with PBS, and the capsule was removed. Each kidney was then weighed individually. Kidneys were

minced into small pieces and enzymatically digested using 1.67 Wunsch U/ml Liberase DL (Roche Diagnostics, Indianapolis, IN) in DMEM medium for 20 minutes at room temperature. PEB buffer (PBS, 2mM EDTA, 0.5% BSA) was added to disrupt calcium-depended cell-cell complexes and to inactivate the Liberase enzyme. Disaggregation was completed by mechanical maceration using frosted glass and the homogenate was passed through a 70-μm nylon filter (Fisher) to remove undigested and fibrogenous material and then centrifuged at 300 g. To remove red blood cells and enrich the renal leukocyte population in the total kidney homogenate, the pellet was suspended in NycoPrep 1.077 gm/ml density gradient solution (Axis-Shield PoC, Oslo, Norway), overlaid with PBS, and centrifuged at 1000 × g for 15 minutes. The interface, containing low-density cells, which includes macrophages and dendritic cells, was collected and washed in PEB buffer for analysis by flow cytometry. For some studies, macrophages were isolated using CD11b magnetic microbeads and MACS columns (Miltenyi Biotec) according to the manufacturer's protocol.

Flow Cytometry

Renal leukocytes were washed with staining buffer (PBS, 0.5% BSA, 0.01% Sodium Azide) and incubated with anti-mouse CD16/32 for 10 minutes on ice to block nonspecific binding of phycoerythrin to FCγ3 receptors. Cells were stained on ice for 30 minutes with 7-aminoactinomycin D (7-AAD, eBioscience) viability staining solution and flurochrome-conjugated anti-mouse antibodies for analysis by flow cytometry. Fluorescein isothicyanate-conjugated CD62L (MEL-14), phycoerythrin-conjugated F4/80 (BM8), allophycocyanin-conjugated major histocompatibility complex class II (MHC II, M5/114.15.2), eFluor 450-conjugated Ly-6C (HK1.4), allophycocyanin-eFluor 780-conjugated Ly-6G (Gr-1, RB6-8C5), and eFluor 605NC-conjugated CD11b (M1/70) were purchased from eBioscience. Brilliant Violet (BV) 785-conjugated CD11c (N418), BV 650-conjugated CD45.1 (A20), and BV 650-conjugated CD45.2 (104) were purchased from Biolegend. Isotype-matched, fluorescently conjugated antibodies of irrelevant specificity were used as controls. Data acquisition was performed on a BD LSR II Flow Cytometer (BD Biosciences). Approximately 6×10^5 live (7-AAD^-) bone marrow-derived ($CD45^+$) events were collected for analysis from each sample. Results were analyzed using FlowJo Software (Tree Star Inc, Ashland, OR). The absolute number of live (7-AAD^-) bone marrow-derived ($CD45^+$) cells per gram of kidney were determined using AccuCheck Counting Beads (Invitrogen, Molecular Probes, Camarillo, CA). The absolute number of the renal leukocyte subsets was determined by the method described by Moon and colleagues (85).

For intracellular cytokine staining, the cells retrieved from NycoPrep density gradient centrifugation were washed once in PBS and then cultured for 4 hours at 37°C and 5% CO2 in DMEM culture media containing 10% FBS and cell stimulation cocktail (PMA/ionomycin) plus protein transport inhibitors (Brefeldin A and Monensin). Next the cells were washed two times in PBS and then stained with fixable viability dye eFluor 520 for 30 minutes at 4C, according to the manufacturer's protocol (eBioscience). The cells were then washed twice with staining buffer and cell surface markers (CD45, CD11b, F4/80, Ly6C, CD11c) were stained, as described above. The cells were then fixed and permeabilized for intracellular cytokine staining according to the manufacturer's protocol (eBioscience). After

staining for intracellular cytokines for 20 minutes at room temperature and 30 minutes on ice, the cells were washed twice with staining buffer and then analyzed on an LSRII flow cytometer.

Quantification of mRNA Expression

Gene expression analysis was performed as described previously (22). Briefly, total RNA was isolated from cells or tissues by TRIzol (Life Technologies), and SYBR Green-based real-time PCR was performed on cDNA product generated from total RNA (Qiagen). Relative mRNA expression was quantified using the ΔΔCt method and normalized to glyceraldehyde 3-phosphate dehydrogenase (GAPDH) mRNA as an internal control. Real-time primers used in this study are described in Table 1. All the reactions were performed in triplicate and specificity was monitored using melting curve analysis.

Isolation and polarization of bone-marrow derived monocytes

BMDMs were isolated and cultured as previously described with minor modifications (38). Mouse bone marrow cells were flushed from the femurs of mice and passed through a 40-μm cell strainer (BD Falcon), and red blood cells were lysed in ACK buffer (0.15 M NH4Cl, 10 mM KHCO3, 0.1 mM EDTA). Remaining cells were incubated in DMEM medium (Corning Cellgro) containing 10% FBS (Atlanta Biologicals), 30 ng/ml MCSF (Miltenyi Biotec) and 1% penicillin/streptomycin (Life Technologies). BMDM were cultured for 7 days and the purity of the culture was determined to be >85% based on analysis of CD11b expression. Polarization of cells was performed using 100 U/ml murine recombinant IFN γ (Roche) or 20 ng/ml murine recombinant IL-4 (Miltenyi Biotec). For studies involving HO by-products or ferritin, pre-treatment was performed 16 hours prior to the addition of cytokines. Macrophages were pre-treated with biliverdin (Frontier Scientific), bilirubin (Frontier Scientific), deferoxamine (Sigma), CORM (Sigma) or Apoferritin (Sigma). Recombinant H ferritin and L ferritin were generously provided by Dr. Arosio. HO-1 overexpressing macrophages were isolated from humanized HO-1 BAC transgenic mice (81). Gene expression analysis was performed at 4 hours and protein expression analysis was performed at 24 hours after cytokine treatment.

Western blot analysis

Harvested cells or collected tissues were lysed in RIPA buffer (50 mmol/l Tris/HCl, 1% NP-40, 0.25%. deoxycholic acid, 150 mmol/l NaCl, 1 mmol/l EGTA, 1 mmol/l sodium orthovanadate, and 1 mmol/l sodium fluoride) with protease inhibitor (Sigma-Aldrich) and quantified using BCA protein assay (Thermo Scientific). Total protein (10–15 μg for cells, 75μg for tissues) was resolved on a 12% Tris-glycine sodium dodecyl sulfate polyacrylamide gel electrophoresis and transferred to a polyvinylidene fluoride membrane (Millipore). Membranes were blocked with 5% nonfat dry milk in PBST for 1 hour and then incubated with a rabbit anti-ferritin H chain antibody (Santa Cruz Biotechnology, 1:5000), a rabbit anti-arginase antibody (Santa Cruz Biotechnology; 1:1000), a rabbit anti-iNOS antibody (Santa Cruz Biotechnology; 1:1000), a rabbit anti-HO-1 antibody (Enzo LifeSciences;1:2000), a rabbit anti-fibronectin (Sigma-Aldrich; 1:10000), a goat anti-L Ferritin (Santa Cruz Biotechnology; 1:1000), or a mouse anti-SMA (Sigma-Aldrich; 1:5000) followed by a peroxidase-conjugated goat anti-rabbit (or mouse) IgG antibody or donkey

anti-goat IgG antibody (Jackson ImmunoResearch Laboratories; 1:10000). Horseradish peroxidase activity was detected using enhanced chemiluminescence detection system (GE Healthcare). The membrane was stripped and probed with anti-GAPDH antibody (Sigma-Aldrich; 1:5000) to confirm loading and transfer. Densitometry analysis was performed and results were normalized to GAPDH expression and expressed as fold change over controls.

Statistics

Data are presented as mean ± SEM. The unpaired Student's t test was used for comparisons between two groups. For comparisons that involved more than two groups, ANOVA and the Newman-Keuls test were used for analysis. All results were considered significant at $P<0.05$. All the experiments were performed at least three times.

Study approval

All procedures involving mice were performed in accordance with NIH guidelines for the use and care of live animals and were reviewed and approved by the Institutional Animal Care and Use Committee (IACUC) of the University of Alabama at Birmingham.

Supplementary Material

Refer to Web version on PubMed Central for supplementary material.

Acknowledgments

We thank Dr. Paolo Arosio for the recombinant H ferritin and the Comprehensive Flow Cytometry Core of the University of Alabama at Birmingham (funded through NIH grants P30 AR048311 and P30 AI027767) for assistance with flow cytometry. We appreciate the technical assistance of Lingling Guo and Daniel McFalls. We thank Dr. Volker Haase for the PEPCK-Cre mice and Dr. Deepak Darshan and Dr. Lukas Kuhn for the $FtH^{Lox/Lox}$ mice. This work was supported by NIH grants (R01 DK59600 to A. Agarwal), the core resource of the UAB-UCSD O'Brien Center (P30 DK079337 to A. Agarwal), R01 DK083390 (to A. Agarwal and J.F. George), Fundacao para a Ciencia e Tecnologia grants (PTDC/SAU-TOX/116627/2010, HMSP-ICT/0022/2010 to M.P. Soares), the European Union grant (ERC-2011-AdG. 294709 DAMAGECONTROL to M.P. Soares) and AHA grant 11POST7600074 (to S. Bolisetty).

References

1. Liu Y. Renal fibrosis: new insights into the pathogenesis and therapeutics. Kidney international. 2006; 69:213–217. [PubMed: 16408108]
2. Strutz F, Neilson EG. New insights into mechanisms of fibrosis in immune renal injury. Springer Semin Immunopathol. 2003; 24:459–476. [PubMed: 12778339]
3. Zeisberg M, Neilson EG. Mechanisms of tubulointerstitial fibrosis. J Am Soc Nephrol. 2010; 21:1819–1834. [PubMed: 20864689]
4. Aksu U, Demirci C, Ince C. The pathogenesis of acute kidney injury and the toxic triangle of oxygen, reactive oxygen species and nitric oxide. Contrib Nephrol. 2011; 174:119–128. [PubMed: 21921616]
5. Sharfuddin AA, Molitoris BA. Pathophysiology of ischemic acute kidney injury. Nature reviews. Nephrology. 2011; 7:189–200. [PubMed: 21364518]
6. Basile DP, Anderson MD, Sutton TA. Pathophysiology of acute kidney injury. Compr Physiol. 2012; 2:1303–1353. [PubMed: 23798302]
7. Kinsey GR, Okusa MD. Role of leukocytes in the pathogenesis of acute kidney injury. Crit Care. 2012; 16:214. [PubMed: 22429752]

8. Furuichi K, Kaneko S, Wada T. Chemokine/chemokine receptor-mediated inflammation regulates pathologic changes from acute kidney injury to chronic kidney disease. Clin Exp Nephrol. 2009; 13:9–14. [PubMed: 19085040]
9. Jang HS, Kim JI, Han SJ, et al. The recruitment and subsequent proliferation of bone marrow-derived cells in postischemic kidney are important to the progression of fibrosis. Am J Physiol Renal Physiol. 2014
10. Koyner JL, Sher Ali R, Murray PT. Antioxidants. Do they have a place in the prevention or therapy of acute kidney injury? Nephron Exp Nephrol. 2008; 109:e109–e117. [PubMed: 18802373]
11. Heyman SN, Rosen S, Rosenberger C. A role for oxidative stress. Contrib Nephrol. 2011; 174:138–148. [PubMed: 21921618]
12. Nath KA. Heme oxygenase-1: a provenance for cytoprotective pathways in the kidney and other tissues. Kidney international. 2006; 70:432–443. [PubMed: 16775600]
13. Lee DW, Faubel S, Edelstein CL. Cytokines in acute kidney injury (AKI). Clin Nephrol. 2011; 76:165–173. [PubMed: 21888852]
14. Akcay A, Nguyen Q, Edelstein CL. Mediators of inflammation in acute kidney injury. Mediators Inflamm. 2009; 2009:137072. [PubMed: 20182538]
15. Kinsey GR, Li L, Okusa MD. Inflammation in acute kidney injury. Nephron Exp Nephrol. 2008; 109:e102–e107. [PubMed: 18802372]
16. Nath KA. Heme oxygenase-1 and acute kidney injury. Curr Opin Nephrol Hypertens. 2014; 23:17–24. [PubMed: 24275768]
17. Wei Q, Hill WD, Su Y, et al. Heme oxygenase-1 induction contributes to renoprotection by G-CSF during rhabdomyolysis-associated acute kidney injury. Am J Physiol Renal Physiol. 2011; 301:F162–F170. [PubMed: 21511696]
18. Bolisetty S, Traylor AM, Kim J, et al. Heme oxygenase-1 inhibits renal tubular macroautophagy in acute kidney injury. J Am Soc Nephrol. 2010; 21:1702–1712. [PubMed: 20705711]
19. Shiraishi F, Curtis LM, Truong L, et al. Heme oxygenase-1 gene ablation or expression modulates cisplatin-induced renal tubular apoptosis. Am J Physiol Renal Physiol. 2000; 278:F726–F736. [PubMed: 10807584]
20. Agarwal A, Balla J, Alam J, et al. Induction of heme oxygenase in toxic renal injury: a protective role in cisplatin nephrotoxicity in the rat. Kidney international. 1995; 48:1298–1307. [PubMed: 8569092]
21. Nath KA, Balla G, Vercellotti GM, et al. Induction of heme oxygenase is a rapid, protective response in rhabdomyolysis in the rat. J Clin Invest. 1992; 90:267–270. [PubMed: 1634613]
22. Zarjou A, Bolisetty S, Joseph R, et al. Proximal tubule H-ferritin mediates iron trafficking in acute kidney injury. J Clin Invest. 2013; 123:4423–4434. [PubMed: 24018561]
23. Gozzelino R, Soares MP. Coupling heme and iron metabolism via ferritin H chain. Antioxid Redox Signal. 2014; 20:1754–1769. [PubMed: 24124891]
24. Zhang MZ, Yao B, Yang S, et al. CSF-1 signaling mediates recovery from acute kidney injury. J Clin Invest. 2012; 122:4519–4532. [PubMed: 23143303]
25. Winterberg PD, Wang Y, Lin KM, et al. Reactive oxygen species and IRF1 stimulate IFNalpha production by proximal tubules during ischemic AKI. Am J Physiol Renal Physiol. 2013; 305:F164–F172. [PubMed: 23657854]
26. Anders HJ, Vielhauer V, Schlondorff D. Chemokines and chemokine receptors are involved in the resolution or progression of renal disease. Kidney international. 2003; 63:401–415. [PubMed: 12631106]
27. Li L, Okusa MD. Macrophages, dendritic cells, and kidney ischemia-reperfusion injury. Semin Nephrol. 2010; 30:268–277. [PubMed: 20620671]
28. Alikhan MA, Ricardo SD. Mononuclear phagocyte system in kidney disease and repair. Nephrology (Carlton). 2013; 18:81–91. [PubMed: 23194390]
29. Williams TM, Little MH, Ricardo SD. Macrophages in renal development, injury, and repair. Semin Nephrol. 2010; 30:255–267. [PubMed: 20620670]

30. Cao Q, Wang Y, Harris DC. Pathogenic and protective role of macrophages in kidney disease. Am J Physiol Renal Physiol. 2013; 305:F3–F11. [PubMed: 23637206]
31. Eardley KS, Zehnder D, Quinkler M, et al. The relationship between albuminuria, MCP-1/CCL2, and interstitial macrophages in chronic kidney disease. Kidney Int. 2006; 69:1189–1197. [PubMed: 16609683]
32. Lim AK, Tesch GH. Inflammation in diabetic nephropathy. Mediators Inflamm. 2012; 2012:146–154.
33. Yang N, Isbel NM, Nikolic-Paterson DJ, et al. Local macrophage proliferation in human glomerulonephritis. Kidney Int. 1998; 54:143–151. [PubMed: 9648072]
34. Chaves LD, Mathew L, Shakaib M, et al. Contrasting effects of systemic monocyte/macrophage and CD4+ T cell depletion in a reversible ureteral obstruction mouse model of chronic kidney disease. Clin Dev Immunol. 2013; 2013:836–989.
35. Henderson NC, Mackinnon AC, Farnworth SL, et al. Galectin-3 expression and secretion links macrophages to the promotion of renal fibrosis. Am J Pathol. 2008; 172:288–298. [PubMed: 18202187]
36. Ko GJ, Boo CS, Jo SK, et al. Macrophages contribute to the development of renal fibrosis following ischaemia/reperfusion-induced acute kidney injury. Nephrol Dial Transplant. 2008; 23:842–852. [PubMed: 17984109]
37. Machida Y, Kitamoto K, Izumi Y, et al. Renal fibrosis in murine obstructive nephropathy is attenuated by depletion of monocyte lineage, not dendritic cells. J Pharmacol Sci. 2010; 114:464–473. [PubMed: 21127386]
38. Lee S, Huen S, Nishio H, et al. Distinct macrophage phenotypes contribute to kidney injury and repair. J Am Soc Nephrol. 2011; 22:317–326. [PubMed: 21289217]
39. Nishida M, Okumura Y, Fujimoto S, et al. Adoptive transfer of macrophages ameliorates renal fibrosis in mice. Biochem Biophys Res Commun. 2005; 332:11–16. [PubMed: 15896292]
40. Martinez FO, Sica A, Mantovani A, et al. Macrophage activation and polarization. Front Biosci. 2008; 13:453–461. [PubMed: 17981560]
41. Mantovani A, Biswas SK, Galdiero MR, et al. Macrophage plasticity and polarization in tissue repair and remodelling. J Pathol. 2013; 229:176–185. [PubMed: 23096265]
42. Sica A, Mantovani A. Macrophage plasticity and polarization: in vivo veritas. J Clin Invest. 2012; 122:787–795. [PubMed: 22378047]
43. Cassetta L, Cassol E, Poli G. Macrophage polarization in health and disease. Scientific World Journal. 2011; 11:2391–2402. [PubMed: 22194670]
44. Biswas SK, Mantovani A. Orchestration of metabolism by macrophages. Cell Metab. 2012; 15:432–437. [PubMed: 22482726]
45. Sierra-Filardi E, Vega MA, Sanchez-Mateos P, et al. Heme Oxygenase-1 expression in M-CSF-polarized M2 macrophages contributes to LPS-induced IL-10 release. Immunobiology. 2010; 215:788–795. [PubMed: 20580464]
46. Durante W. Protective role of heme oxygenase-1 against inflammation in atherosclerosis. Front Biosci (Landmark Ed). 2011; 16:2372–2388. [PubMed: 21622183]
47. Paine A, Eiz-Vesper B, Blasczyk R, et al. Signaling to heme oxygenase-1 and its anti-inflammatory therapeutic potential. Biochem Pharmacol. 2010; 80:1895–1903. [PubMed: 20643109]
48. Hull TD, Agarwal A, George JF. The mononuclear phagocyte system in homeostasis and disease: a role for heme oxygenase-1. Antioxid Redox Signal. 2014; 20:1770–1788. [PubMed: 24147608]
49. Li L, Huang L, Sung SS, et al. The chemokine receptors CCR2 and CX3CR1 mediate monocyte/macrophage trafficking in kidney ischemia-reperfusion injury. Kidney international. 2008; 74:1526–1537. [PubMed: 18843253]
50. Sunderkotter C, Nikolic T, Dillon MJ, et al. Subpopulations of mouse blood monocytes differ in maturation stage and inflammatory response. J Immunol. 2004; 172:4410–4417. [PubMed: 15034056]
51. Tacke F, Randolph GJ. Migratory fate and differentiation of blood monocyte subsets. Immunobiology. 2006; 211:609–618. [PubMed: 16920499]

52. Nahrendorf M, Swirski FK. Monocyte and macrophage heterogeneity in the heart. Circ Res. 2013; 112:1624–1633. [PubMed: 23743228]
53. Davies LC, Jenkins SJ, Allen JE, et al. Tissue-resident macrophages. Nat Immunol. 2013; 14:986–995. [PubMed: 24048120]
54. Kawakami T, Lichtnekert J, Thompson LJ, et al. Resident renal mononuclear phagocytes comprise five discrete populations with distinct phenotypes and functions. J Immunol. 2013; 191:3358–3372. [PubMed: 23956422]
55. Kie JH, Kapturczak MH, Traylor A, et al. Heme oxygenase-1 deficiency promotes epithelial-mesenchymal transition and renal fibrosis. J Am Soc Nephrol. 2008; 19:1681–1691. [PubMed: 18495963]
56. Ferreira C, Bucchini D, Martin ME, et al. Early embryonic lethality of H ferritin gene deletion in mice. J Biol Chem. 2000; 275:3021–3024. [PubMed: 10652280]
57. Chovatiya R, Medzhitov R. Stress, inflammation, and defense of homeostasis. Mol Cell. 2014; 54:281–288. [PubMed: 24766892]
58. Biswas SK, Chittezhath M, Shalova IN, et al. Macrophage polarization and plasticity in health and disease. Immunol Res. 2012; 53:11–24. [PubMed: 22418728]
59. Hume DA. Applications of myeloid-specific promoters in transgenic mice support in vivo imaging and functional genomics but do not support the concept of distinct macrophage and dendritic cell lineages or roles in immunity. J Leukoc Biol. 2011; 89:525–538. [PubMed: 21169519]
60. Levi S, Arosio P. Mitochondrial ferritin. Int J Biochem Cell Biol. 2004; 36:1887–1889. [PubMed: 15203103]
61. Drysdale J, Arosio P, Invernizzi R, et al. Mitochondrial ferritin: a new player in iron metabolism. Blood Cells Mol Dis. 2002; 29:376–383. [PubMed: 12547228]
62. Linsenmayer TF, Cai CX, Millholland JM, et al. Nuclear ferritin in corneal epithelial cells: tissue-specific nuclear transport and protection from UV-damage. Prog Retin Eye Res. 2005; 24:139–159. [PubMed: 15610971]
63. Surguladze N, Patton S, Cozzi A, et al. Characterization of nuclear ferritin and mechanism of translocation. Biochem J. 2005; 388:731–740. [PubMed: 15675895]
64. Thompson KJ, Fried MG, Ye Z, et al. Regulation, mechanisms and proposed function of ferritin translocation to cell nuclei. J Cell Sci. 2002; 115:2165–2177. [PubMed: 11973357]
65. Harrison PM, Arosio P. The ferritins: molecular properties, iron storage function and cellular regulation. Biochim Biophys Acta. 1996; 1275:161–203. [PubMed: 8695634]
66. Gozzelino R, Andrade BB, Larsen R, et al. Metabolic adaptation to tissue iron overload confers tolerance to malaria. Cell Host Microbe. 2012; 12:693–704. [PubMed: 23159058]
67. Rosario C, Zandman-Goddard G, Meyron-Holtz EG, et al. The hyperferritinemic syndrome: macrophage activation syndrome, Still's disease, septic shock and catastrophic antiphospholipid syndrome. BMC Med. 2013; 11:185. [PubMed: 23968282]
68. Recalcati S, Invernizzi P, Arosio P, et al. New functions for an iron storage protein: the role of ferritin in immunity and autoimmunity. J Autoimmun. 2008; 30:84–89. [PubMed: 18191543]
69. Morikawa K, Oseko F, Morikawa S. H- and L-rich ferritins suppress antibody production, but not proliferation, of human B lymphocytes in vitro. Blood. 1994; 83:737–743. [PubMed: 8298135]
70. Hann HW, Stahlhut MW, Lee S, et al. Effects of isoferritins on human granulocytes. Cancer. 1989; 63:2492–2496. [PubMed: 2720599]
71. Gray CP, Franco AV, Arosio P, et al. Immunosuppressive effects of melanomaderived heavy-chain ferritin are dependent on stimulation of IL-10 production. Int J Cancer. 2001; 92:843–850. [PubMed: 11351305]
72. Davis CL, Kausz AT, Zager RA, et al. Acute renal failure after cardiopulmonary bypass in related to decreased serum ferritin levels. J Am Soc Nephrol. 1999; 10:2396–2402. [PubMed: 10541300]
73. Ruddell RG, Hoang-Le D, Barwood JM, et al. Ferritin functions as a proinflammatory cytokine via iron-independent protein kinase C zeta/nuclear factor kappaB-regulated signaling in rat hepatic stellate cells. Hepatology. 2009; 49:887–900. [PubMed: 19241483]
74. Dai Y, Zhang W, Wen J, et al. A2B adenosine receptor-mediated induction of IL-6 promotes CKD. J Am Soc Nephrol. 2011; 22:890–901. [PubMed: 21511827]

75. Pesce JT, Ramalingam TR, Mentink-Kane MM, et al. Arginase-1-expressing macrophages suppress Th2 cytokine-driven inflammation and fibrosis. PLoS Pathog. 2009; 5:e1000371. [PubMed: 19360123]

76. Meng XM, Nikolic-Paterson DJ, Lan HY. Inflammatory processes in renal fibrosis. Nature reviews. Nephrology. 2014; 10:493–503. [PubMed: 24981817]

77. Vernon MA, Mylonas KJ, Hughes J. Macrophages and renal fibrosis. Seminars in nephrology. 2010; 30:302–317. [PubMed: 20620674]

78. LeBleu VS, Taduri G, O'Connell J, et al. Origin and function of myofibroblasts in kidney fibrosis. Nature medicine. 2013; 19:1047–1053.

79. Kalantar-Zadeh K, Don BR, Rodriguez RA, et al. Serum ferritin is a marker of morbidity and mortality in hemodialysis patients. Am J Kidney Dis. 2001; 37:564–572. [PubMed: 11228181]

80. Rambod M, Kovesdy CP, Kalantar-Zadeh K. Combined high serum ferritin and low iron saturation in hemodialysis patients: the role of inflammation. Clin J Am Soc Nephrol. 2008; 3:1691–1701. [PubMed: 18922994]

81. Kim J, Zarjou A, Traylor AM, et al. In vivo regulation of the heme oxygenase-1 gene in humanized transgenic mice. Kidney international. 2012; 82:278–291. [PubMed: 22495295]

82. Darshan D, Vanoaica L, Richman L, et al. Conditional deletion of ferritin H in mice induces loss of iron storage and liver damage. Hepatology. 2009; 50:852–860. [PubMed: 19492434]

83. Zarjou A, Yang S, Abraham E, et al. Identification of a microRNA signature in renal fibrosis: role of miR-21. Am J Physiol Renal Physiol. 2011; 301:F793–F801. [PubMed: 21775484]

84. Hull TD, Bolisetty S, DeAlmeida AC, et al. Heme oxygenase-1 expression protects the heart from acute injury caused by inducible Cre recombinase. Lab Invest. 2013; 93:868–879. [PubMed: 23732814]

85. Moon JJ, Chu HH, Hataye J, et al. Tracking epitope-specific T cells. Nat Protoc. 2009; 4:565–581. [PubMed: 19373228]

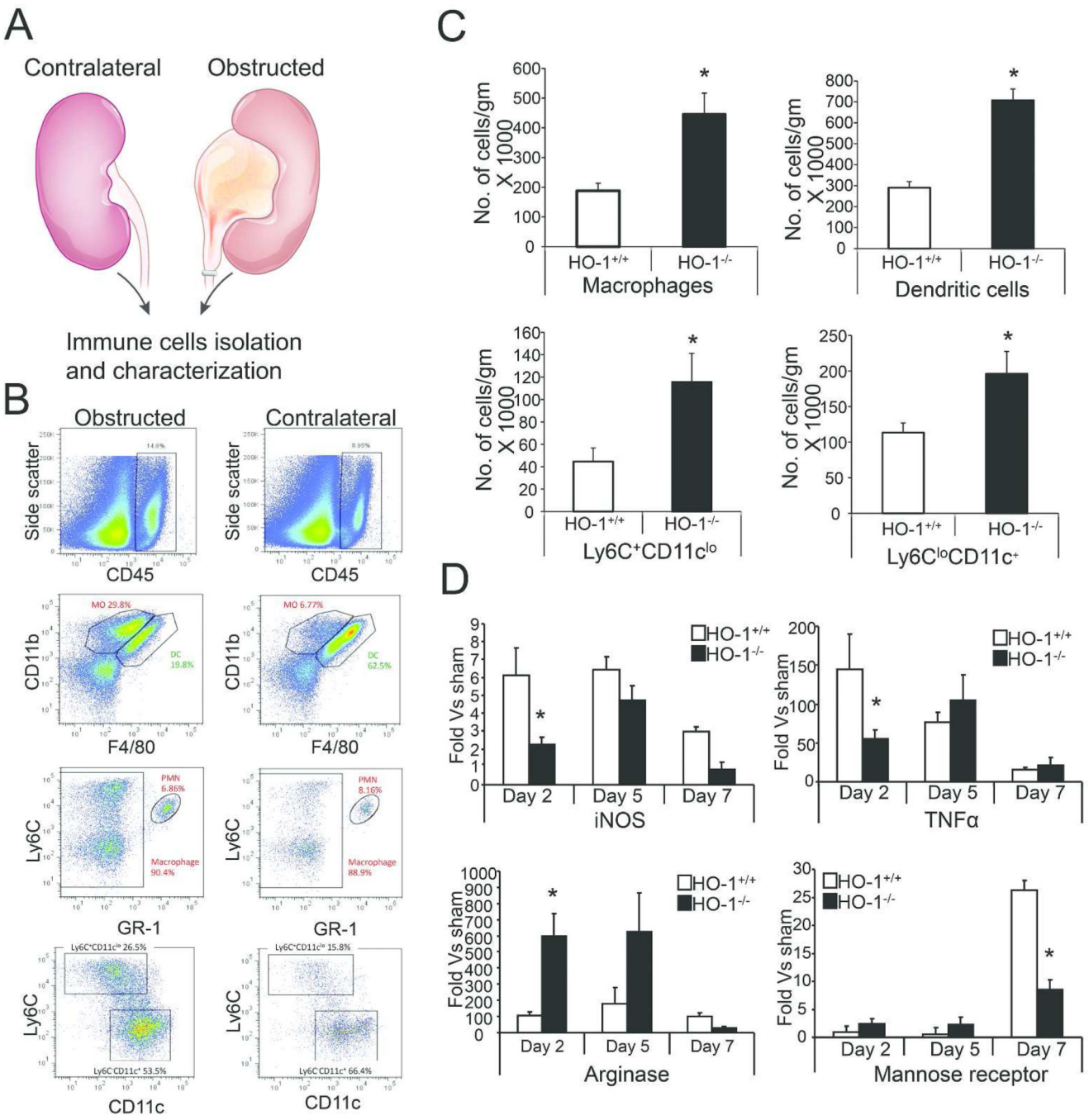

Figure 1. Heme oxygenase-1 (HO-1) deficiency is associated with increased accumulation of immune cells and dysregulated macrophage polarization following unilateral ureteral obstruction (UUO)

(A) Diagram of the injury model. (B) Representative flow cytometry histograms of obstructed and contralateral kidneys demonstrating the gating scheme and proportions of immune cell populations. (C) Quantification of the number of cells in the obstructed kidneys of *HO-1*$^{+/+}$ and *HO-1*$^{-/-}$ mice two days following UUO. Data are represented as number of cells per gram kidney. n=5–8 per group; $p<0.05$ vs *HO-1*$^{+/+}$. Each experiment was performed at least three independent times. (D) Gene expression analysis of polarization

markers (M1: *iNOS*, TNFα; M2: *Arginase*, *Mannose receptor*) on macrophages isolated from obstructed kidneys of *HO-1*$^{+/+}$ and *HO-1*$^{-/-}$ mice at the indicated times following UUO. Data were normalized to sham controls. n=5–8 per group; experiments were repeated three independent times; $p<0.05$ vs *HO-1*$^{+/+}$.

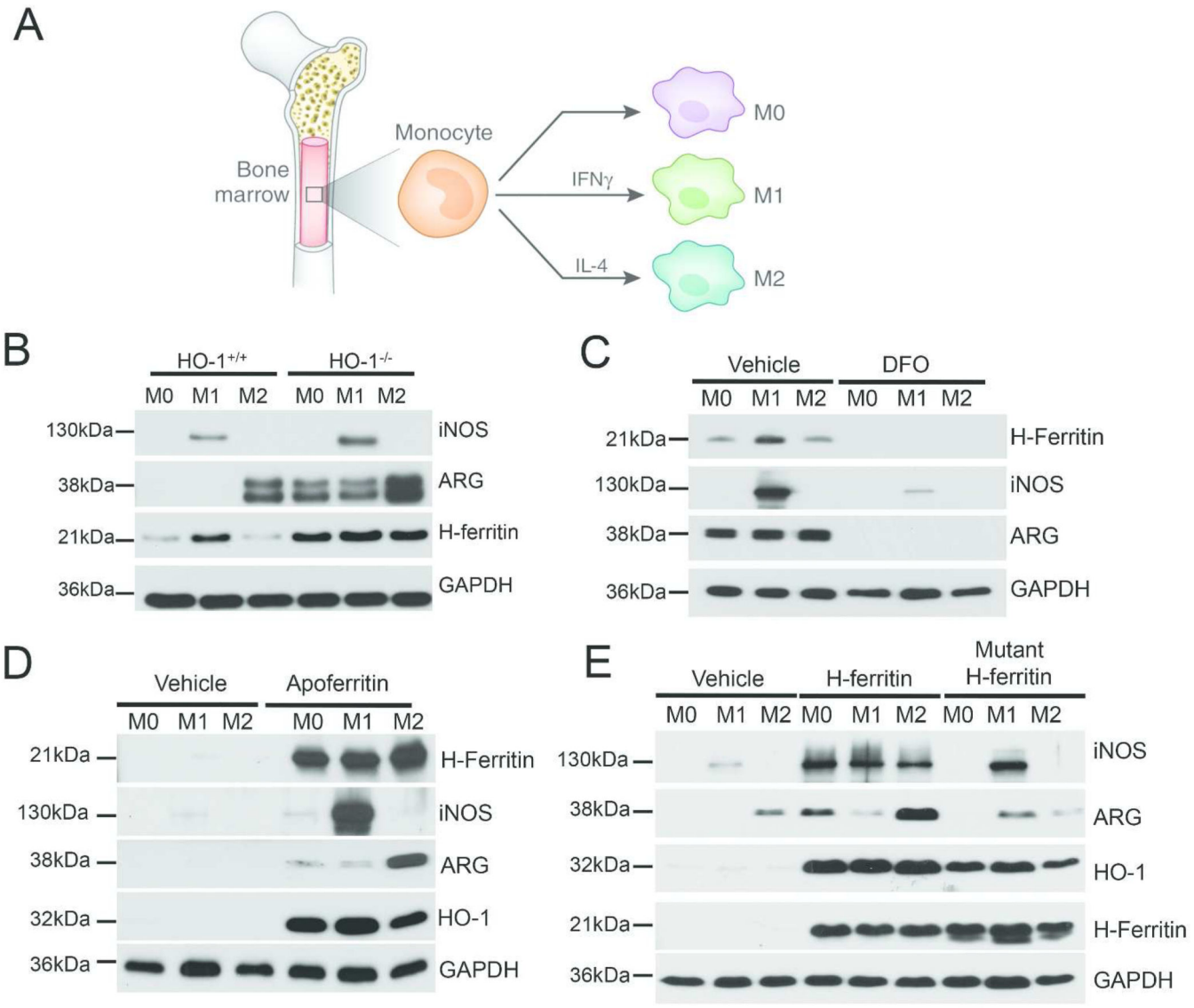

Figure 2. H-Ferritin mediates macrophage polarization

(A) Diagram demonstrates macrophage polarization pathways. (B) *HO-1*$^{+/+}$ and *HO-1*$^{-/-}$ bone marrow-derived monocytes (BMDM) were cultured in vitro in the presence of M-CSF and stimulated with IFNγ (100 U/ml) or IL-4 (20 ng/ml) for 24 h to induce M1 or M2 polarization respectively. Whole cell lysates were analyzed for the expression of iNOS (M1), arginase (M2) and FtH by western blot analysis. Membranes were probed for GAPDH to demonstrate equal loading. (C) HO-1$^{-/-}$ BMDM were pre-treated with vehicle (water) or deferoxamine (DFO; 150 μM) for 16 h prior to stimulation with IFNγ or IL-4. Western analysis was performed for the expression of iNOS, arginase and FtH. (D) HO-1$^{+/+}$ BMDM were pretreated with apoferritin (0.1mg/ml), stimulated with IFNγ or IL-4 and analyzed for the expression of iNOS, arginase, FtH and HO-1 by western blot analysis. (E) HO-1$^{+/+}$ BMDM were pre-treated with H-ferritin or mutant-H-Ferritin, stimulated with IFNγ or IL-4 and analyzed for the expression of iNOS, arginase, FtH, HO-1 and GAPDH by western blot analysis. All experiments were repeated at least three independent times.

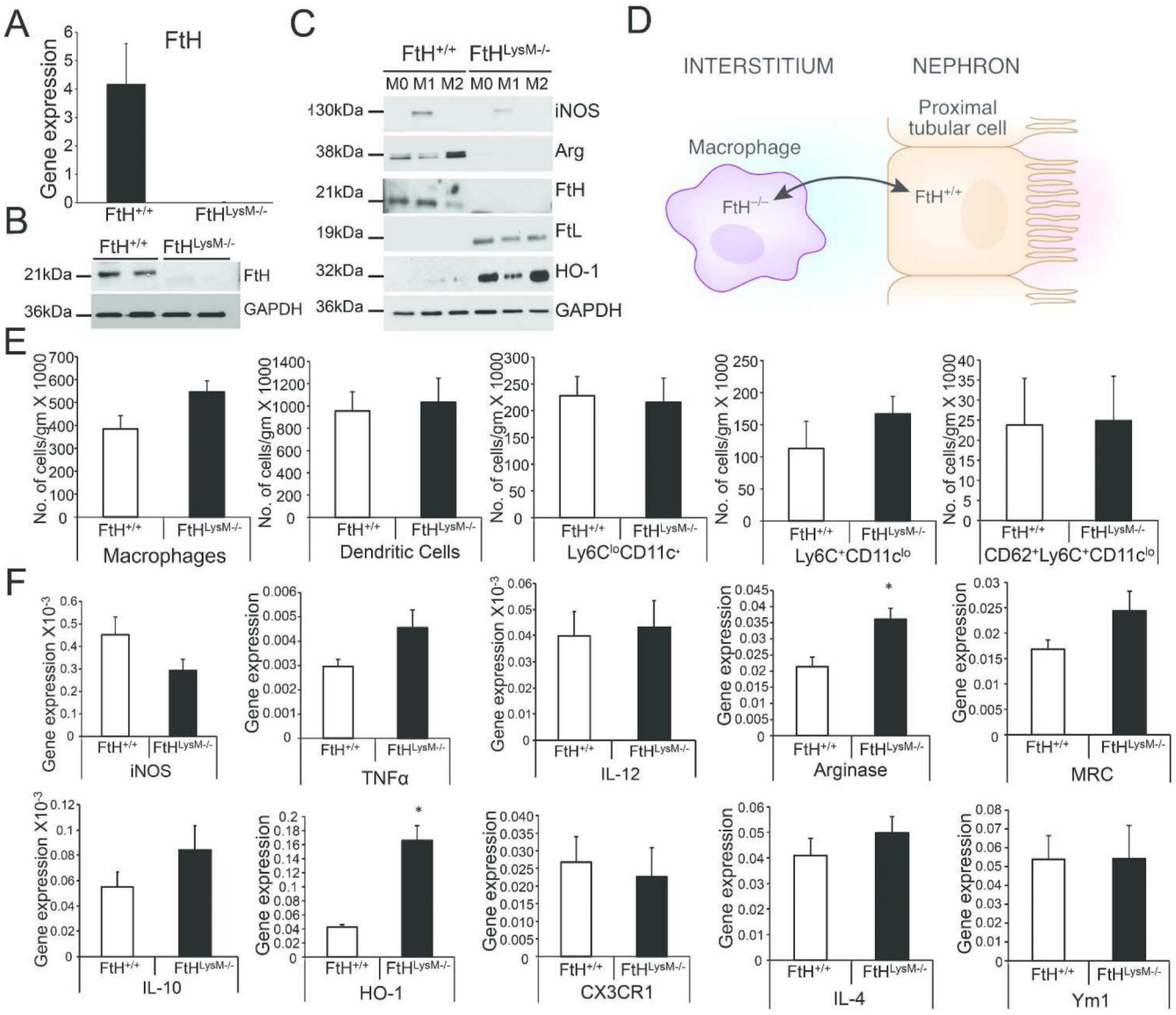

Figure 3. Myeloid-specific FtH deletion does not influence inflammation and macrophage polarization in vivo

(A) FtH mRNA expression in the macrophages of *FtH*$^{+/+}$ and *FtH*$^{\text{LysM}-/-}$ mice was analyzed by real-time PCR. Results are expressed as FtH gene expression normalized to GAPDH. Values are presented as mean ± SEM; *p < 0.05 vs FtH$^{+/+}$. n=3/group. (B) Macrophages isolated from *FtH*$^{+/+}$ and *FtH*$^{\text{LysM}-/-}$ mice were analyzed for FtH protein expression. (C) BMDM from FtH$^{+/+}$ and *FtH*$^{\text{LysM}-/-}$ mice were treated with vehicle (M0), IFNγ (M1) or IL-4 (M2) and analyzed for the expression of iNOS, arginase, FtH, FtL and HO-1 by western blot analysis. Membranes were stripped and re-probed for GAPDH to demonstrate equal loading. (D) Diagram representation of the site-specific expression of FtH in *FtH*$^{\text{LysM}-/-}$ mice. (E) Quantification of the number of cells in the obstructed kidneys of FtH$^{+/+}$ and *FtH*$^{\text{LysM}-/-}$ mice two days following UUO. Data are represented as number of cells per gram kidney. n=4–6 per group; p<0.05 vs FtH$^{+/+}$. Experiments were performed three independent times. (F) Gene expression analysis of polarization markers (M1: *iNOS*,

TNFα, *IL-12*; M2: *Arginase*, *Mannose receptor*, *IL-4*, *Ym1*, *CX3CR1*, *IL-10*) and *HO-1* on macrophages isolated from obstructed kidneys of $FtH^{+/+}$ and $FtH^{LysM-/-}$ mice following UUO. Experiments were performed at least three times and gene expression data were normalized to *GAPDH*, analyzed and represented as mean ± SEM; n=5–8 per group; $p<0.05$ vs $FtH^{+/+}$.

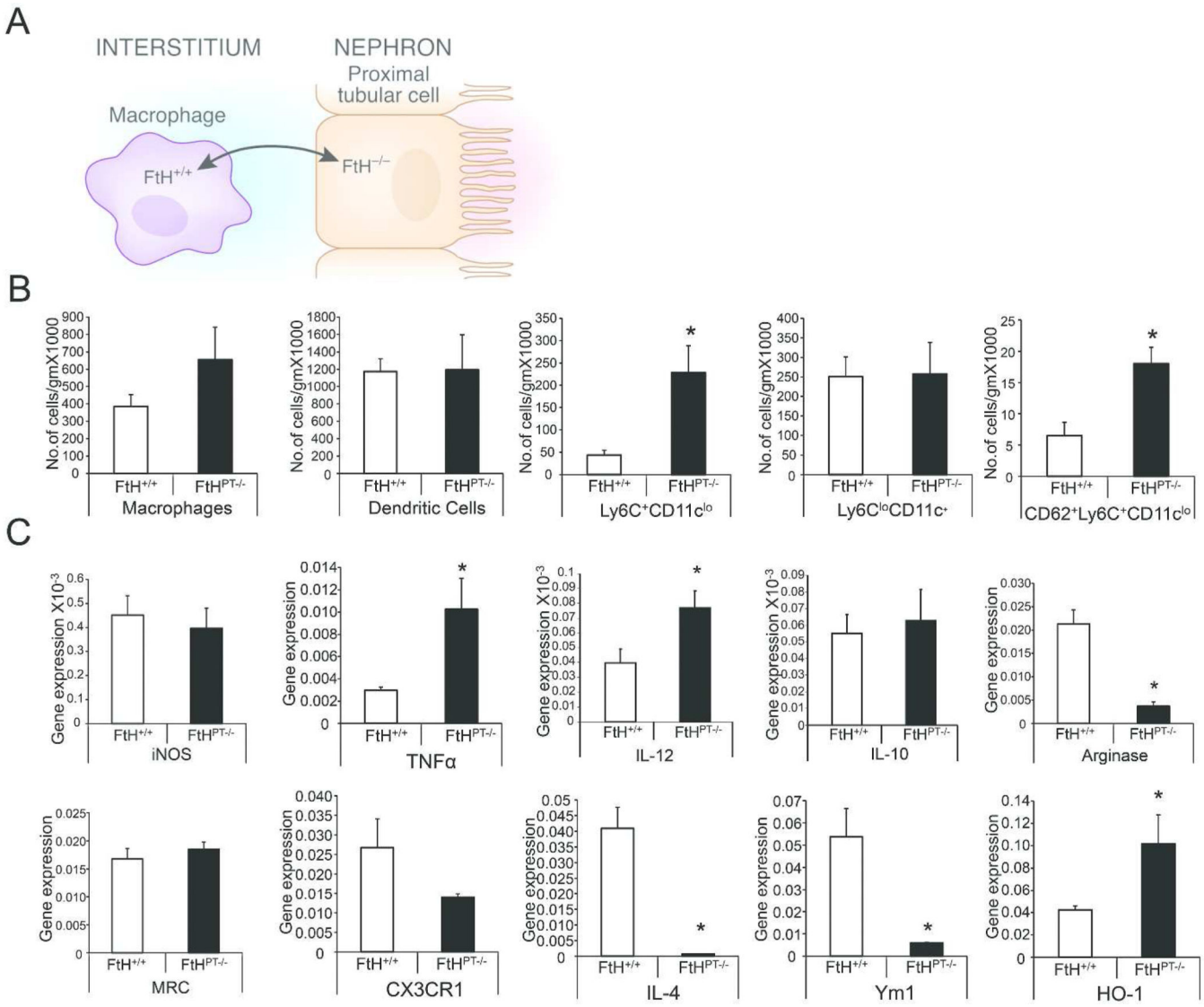

Figure 4. Proximal tubule specific FtH deletion leads to increased macrophage infiltration and altered polarization profile following UUO

(A) Diagram representation of *FtH*$^{PT-/-}$ mice. (B) Two days post UUO, obstructed kidneys of *FtH*$^{+/+}$ and *FtH*$^{PT-/-}$ mice were analyzed for the presence of immune cells by flow cytometry. Data are represented as number of cells per gram kidney. n=4–6 per group; $p < 0.05$ vs *FtH*$^{+/+}$. (C) Macrophages isolated from the obstructed kidneys were analyzed for the expression of, M1 (*iNOS, TNFα, IL-12*), M2 genes (*Arginase, Mannose receptor, IL-4, Ym1, CX3CR1, IL-10*) and *HO-1*. Experiments were performed at least three independent times and gene expression data were normalized to *GAPDH*, analyzed and represented as mean ± SEM; n=5–8 per group; $p<0.05$ vs *FtH*$^{+/+}$.

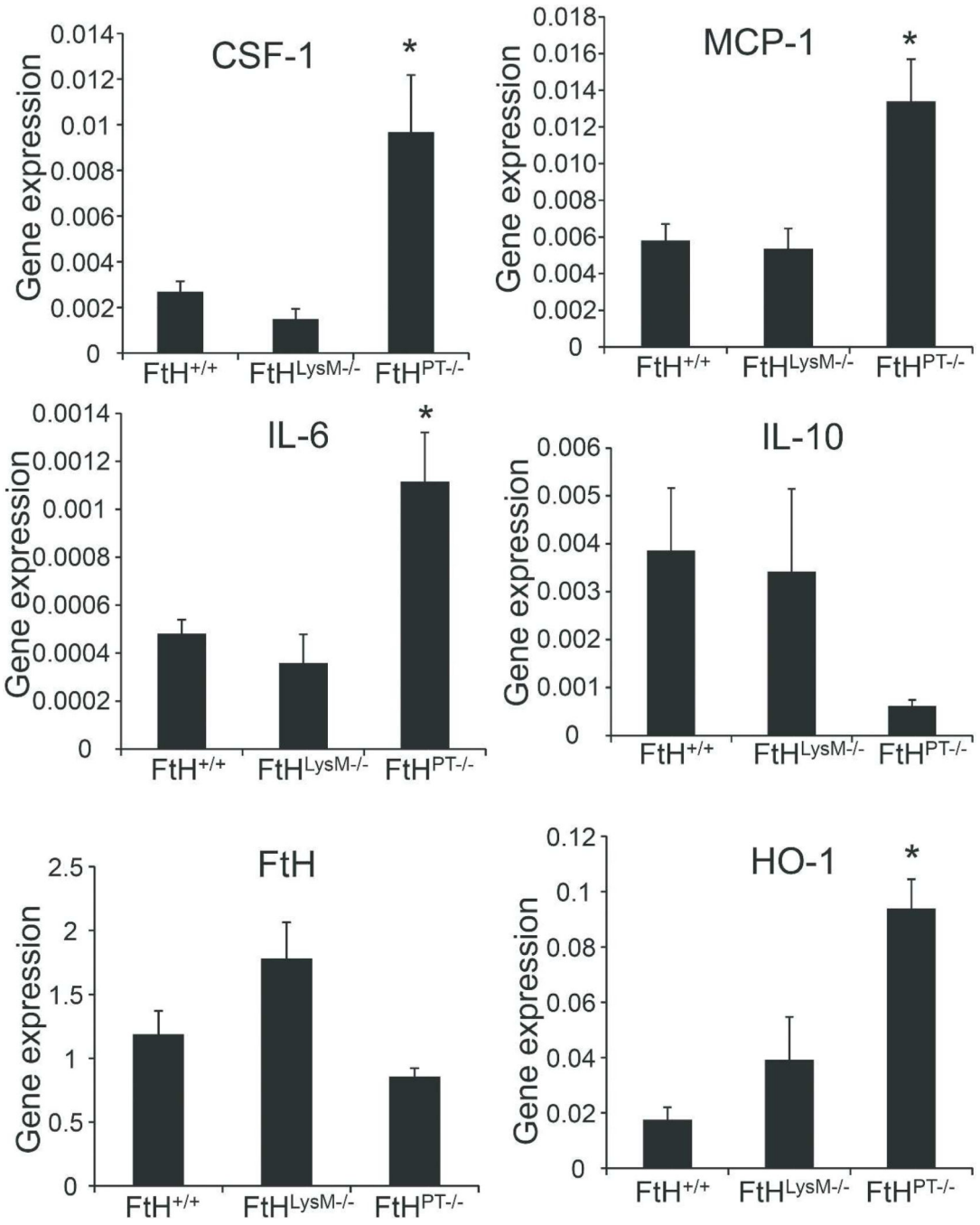

Figure 5. Elucidation of myeloid-specific and proximal tubule-specific H Ferritin deletion on inflammatory chemokines during UUO injury

Two days following UUO, obstructed kidneys of *FtH*$^{+/+}$, *FtH*$^{\text{LysM}-/-}$ and *FtH*$^{\text{PT}-/-}$ mice were analyzed for the expression of chemokines (CSF-1; colony stimulating factor and MCP-1; monocyte chemoattractant protein), inflammatory (IL-6) and anti-inflammatory (IL-10) cytokines and HO-1 and FtH by Real-time PCR analysis. Each experiment was performed at least three independent times. Results were normalized to GAPDH and presented as mean ± SEM; n-4–6 per group. *$p < 0.05$ vs FtH$^{+/+}$ mice.

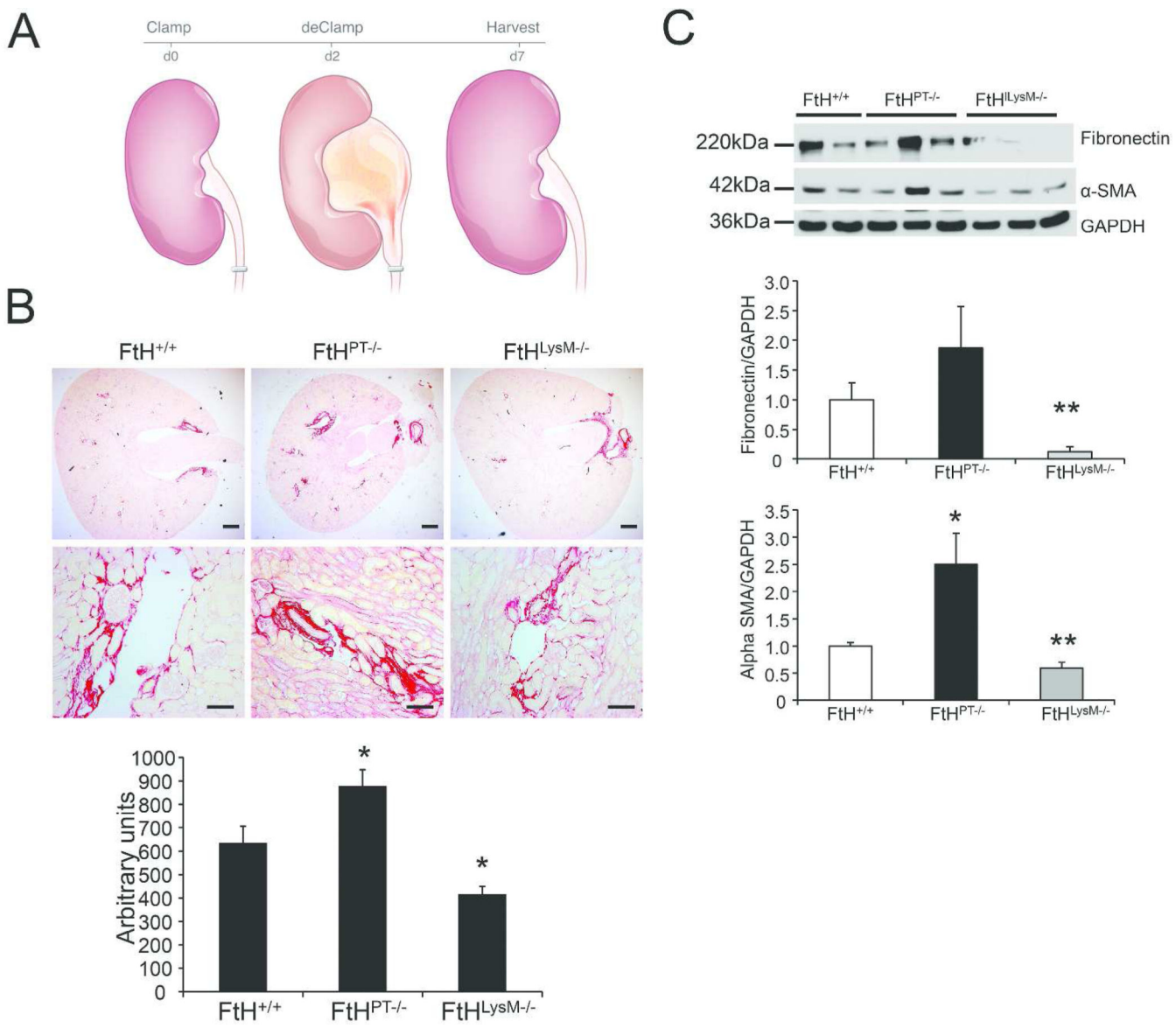

Figure 6. Elucidation of myeloid-specific and proximal tubule-specific H Ferritin deletion on fibrosis during UUO injury

(A) Illustration of experimental design. Two days following clamping of the ureter, the clamp is removed and animals were allowed to recover for five days. (B) Picrosirius staining was performed on the obstructed kidney sections to determine fibrosis following injury. Representative images of the stained kidney sections are shown in the upper panel (scale bar – 400 μm) and middle panel (scale bar – 100 μm). Lower panel: graphical representation of the collagen deposition in the kidneys. *p<0.05 vs $FtH^{+/+}$ mice; n=5–6 per group. Experiment was repeated at least three independent times. (C) Whole kidney lysates from the obstructed kidneys of $FtH^{+/+}$, $FtH^{LysM-/-}$ and $FtH^{PT-/-}$ mice were analyzed for changes in fibrosis (fibronectin and α-smooth muscle actin) by western blot analysis. Expression of the indicated proteins in the kidneys was analyzed by densitometry, normalized to GAPDH

and expressed as mean ± SEM; *p < 0.05 vs $FtH^{+/+}$ mice. **p<0.05 vs $FtH^{PT-/-}$ mice. Experiment was performed using triplicates at least two independent times.

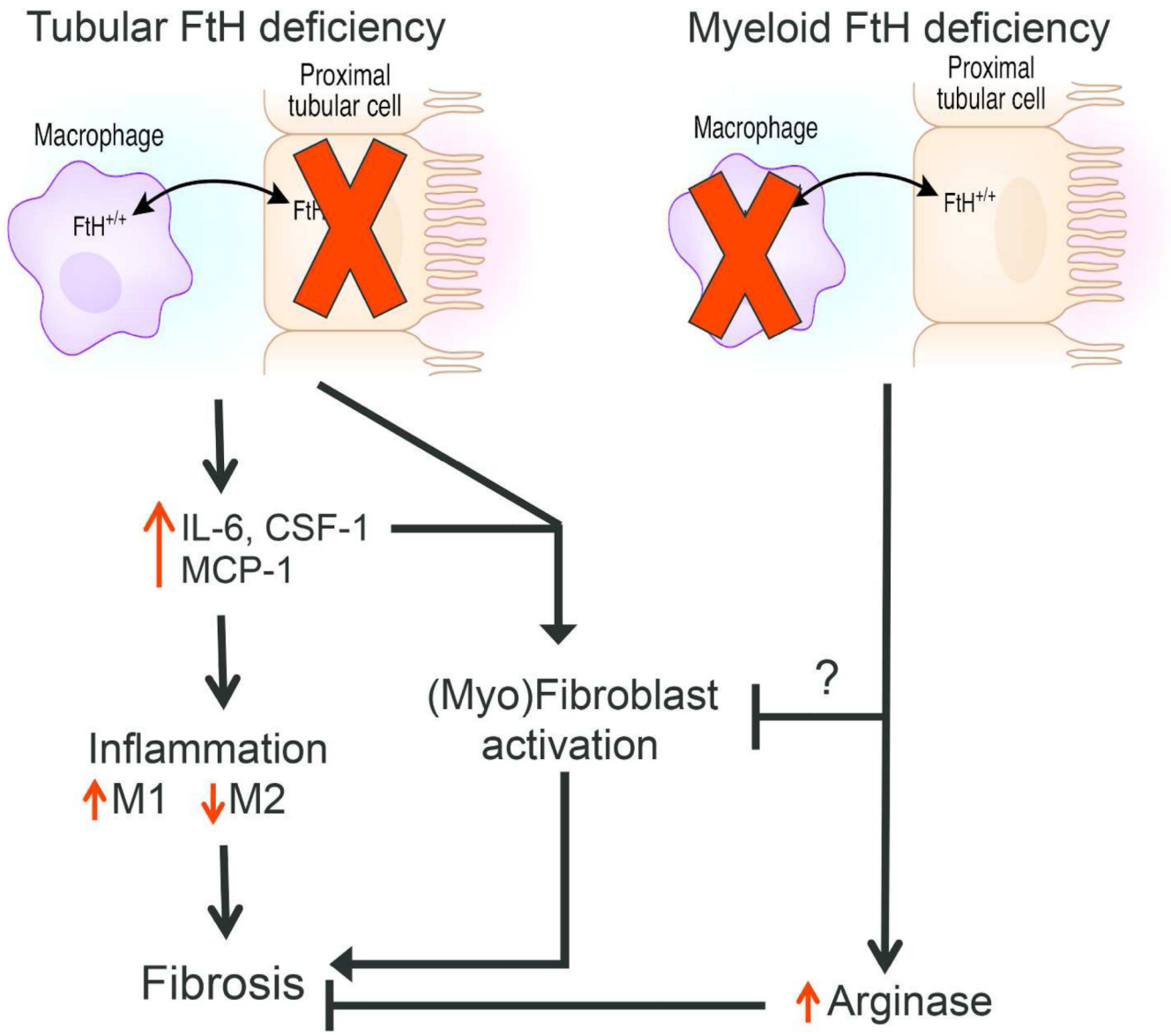

Figure 7. Model depicting the cell-specific effects of FtH in the regulation of inflammation and fibrosis

The absence of FtH in the proximal tubule leads to aggravated injury that comprises of increased generation of chemokines (MCP-1 and CSF-1) and cytokines such as IL-6, followed by an increase in macrophage recruitment and polarization towards the pro-inflammatory phenotype, resulting in increased fibrosis. Increased expression of α-smooth muscle actin may also indicate alternate pathways, including activation of (myo)fibroblasts by the injured epithelium and IL-6. Myeloid FtH deficiency leads to reduced fibrosis following UUO, possibly through mechanisms involving arginase and (myo)fibroblast recruitment and activation.

Table 1

Primers for genotyping and Real-time PCR analysis

Assay	Gene	Primer sequence (5'-3')
Genotyping	H-ferritin flox For	ccatcaaccgccagatcaac
	H-ferritin flox Rev	cgccatactccaggaggaac
	Cre Fwd	gccaggcgttttctgagcatac
	Cre Rev	caccattgcccctgtttcactatc
Real-time PCR	HO-1 Fwd	ggtgatggcttccttgtacc
	HO-1 Rev	agtgaggcccataccagaag
	GAPDH Fwd	atcatccctgcatccact
	GAPDH Rev	atccacgacggacacatt
	L-Ferritin Fwd	cgtctcctcgagtttcagaac
	L-Ferritin Rev	ctcctgggttttaccccattc
	H-Ferritin Fwd	ccatcaaccgccagatcaac
	H-Ferritin Rev	gaaacatcatctcggtcaaa
	Arginase Fwd	ctccaagccaaagtccttagag
	Arginase Rev	aggagctgtcattagggacatc
	iNOS Fwd	ccaagccctcacctacttcc
	iNOS Rev	ctctgagggctgacacaagg
	TNFα Fwd	acggcatggatctcaaagac
	TNFα Rev	agatagcaaatcggctgacg
	MRC Fwd	cctgtgctcgagaggatatg
	MRC Rev	gcagtctgcataccacttgt
	Ym1 Fwd	ttcttgtcacaggtctgg
	Ym1 Rev	tccttagcccaactggtatag
	IL-4 Fwd	gagactctttcgggcttttc
	IL-4 Rev	tgatgctctttaggctttcca
	CX3CR1 Fwd	tcccttcccatctgctcag
	CX3CR1 Rev	acaatgtcgcccaaataacagg
	CSF-1 Fwd	cgggcatcatcctagtcttgctgactgt
	CSF-1 Rev	atagtggcagtatgtgggggcatcctc
	IL-6 Fwd	ctgcaagagacttccatccag
	IL-6 Rev	agtggtatagacaggtctgttgg
	IL-10 Fwd	gctcttactgactggcatgag
	IL-10 Rev	cgcagctctaggagcatgtg
	MCP-1 Fwd	actcacctgctgctactcat
	MCP-1 Rev	ctacagcttctttgggaca